ON-LINE APPENDIX: EXPANDED METHODS AND RESULTS

Accuracy of Volume Pulsation Quantification

In this Appendix, we further explain in detail how we studied the accuracy of the volume pulsation quantification analysis. The workflow is graphically supported by the flowchart in On-line Fig 1.

The Effect of Contrast-to-Noise Ratio and Signal Intensity Fluctuations on the Accuracy of the Pulsation Analysis and the Interaction with Aneurysm Size

In images with low CNR, the difference in intensity between the aneurysm and the background can be small. When one uses a signal intensity–based segmentation method, the aneurysm volumes in these low CNR images could be overestimated. These artifactual volume changes resulting from signal fluctuations and low CNR are due to a change in the detection of the border and thus depend on the size of the aneurysm or object.

Some systematic signal fluctuations over the heartbeat that are intrinsic to the acquisition method cannot be excluded, though these fluctuations were minimized using cardiac gating in the TFE sequence, which means that the signal was maintained in steady-state while waiting for the next electrocardiogram R wave. Such signal fluctuations could be interpreted as a volume change by our segmentation method.

To study the effect of CNR and signal intensity fluctuations on the accuracy of the pulsation analysis, we simulated a spheric static digital phantom in Matlab R2013b (MathWorks, Natick, Massachusetts). A graphical user interface was built to perform image analysis similar to the segmentation method used in the patient study (Analyze). The ROI for segmentation of the phantom volume was standardized at twice the size of the phantom, and the signal intensity threshold for segmentation was chosen manually. To avoid the need for manual corrections of falsely included or excluded voxels after segmentation, we added a connected component analysis and a filling process to the image analysis. Using connected component analysis, we preserved the largest area of connected voxels in the image while discarding all other single voxels. In the filling process, excluded pixels in the lumen of the phantom were automatically filled.

Contrast-to-Noise Ratio

To address the inaccuracy due to noise, we created images with decreasing contrast-to-noise ratios. A static phantom with a diameter of 14 mm (volume = 1500 mm^3) was used, and noise was added using the Rice distribution to simulate MR imaging characteristic noise.[1] Various amounts of noise were added to let the SNR of the phantom range in 15 steps between approximately 3 and 40.

Absolute (in cubic millimeters) and relative volume pulsations were measured in the static phantoms in which CNR was varied, further referred to as the "estimated inaccuracy of the volume pulsation analysis."

The results of this analysis showed that the effect of CNR on the estimated inaccuracy increases quickly below a CNR of approximately 6 (On-line Fig 2).

Interaction of the Contrast-to-Noise Ratio with Aneurysm Size (Phantom Volume) and Its Effect on the Accuracy of the Pulsation Analysis

The interaction of noise with the volume of the static phantom was analyzed for 3 different CNRs: high (CNR≈12), medium (CNR≈4), and low (CNR≈2) CNR. Eleven static phantoms with increasing volumes (range, 12–1500 mm^3) were used to study the interaction of CNR and aneurysm size (phantom volume). In these phantoms, the absolute (in cubic millimeters) and relative volume pulsation was measured. The results of this analysis showed that in high-CNR images, the image analysis performs flawlessly and independent of phantom size (On-line Fig 3). In the phantoms with medium CNR, the estimated inaccuracy was small. The absolute estimated inaccuracy linearly increased with increasing phantom size (On-line Fig 3*A*). When one analyzed the relative influence, a steep increase in estimated inaccuracy with decreasing phantom size was seen (On-line Fig 3*B*). Similar results were found in the phantom with low CNR but with considerably larger absolute and relative inaccuracies (On-line Fig 3).

Signal Intensity Fluctuations

To address the inaccuracy due to signal intensity fluctuations, we multiplied the static basic phantom intensity with a sine to create a sinusoidal intensity fluctuation throughout the 15 time phases. The magnitude of the sine varied between 0% and 10% of the mean intensity of the phantom. In this analysis, the CNR level was kept high, with a mean CNR of 12. To simulate the MR images and the inflow effect of blood realistically, we introduced a partial volume effect to the phantom images. First, a high-resolution phantom with 0.05-mm isotropic resolution (ie, each voxel in the final phantom image contained 11 × 11 × 11 voxels in the high-resolution phantom) was rendered. Using fast Fourier transform, we converted this high-resolution phantom from the spatial to the frequency domain (*k*-space). The *k*-space was cropped back to the original resolution. Subsequently, the cropped *k*-space was transformed back to the spatial domain using the inverse fast Fourier transform (On-line Fig 4). Finally, noise was added to the image, and image analysis was performed.

Absolute (in cubic millimeters) and relative volume pulsations were measured in the static phantoms in which signal intensity was varied, further referred to as the estimated inaccuracy of the volume pulsation analysis. The results of this analysis showed that estimated inaccuracy increased with increasing intensity fluctuation (On-line Fig 5).

Interaction of Signal Intensity Fluctuations with Aneurysm Size (Phantom Volume) and Its Effect on the Accuracy of the Pulsation Analysis

The interaction of phantom volume with the inaccuracy due to intensity fluctuations was also analyzed. This analysis was performed on the static phantom with 3 different sizes (large, volume = 1500 mm^3; medium, volume = 460 mm^3; and small, volume of 12 mm^3).

The results of the analysis of the interaction of size with intensity fluctuations are shown in On-line Fig 5. The larger the phantom volume, the larger was the absolute pulsation in the phantom (in cubic millimeters, On-line Fig 5*A*). However, when one looked at

relative pulsation, small phantoms had a relatively larger inaccuracy than the larger phantoms (On-line Fig 5*B*).

Estimation of Aneurysm-Specific Inaccuracy

As shown with the phantom measurements, both signal intensity fluctuations and CNR play a role in the inaccuracy of the measurement of actual aneurysm pulsation, and this inaccuracy depends on the size of the phantom. To estimate the inaccuracy of each of the pulsation measurements in the patient study in Stages I and II, we performed an additional phantom experiment.

Patient-specific pulsating phantoms were created using an optimized version of the graphical user interface built to create static phantoms in Matlab (described above). The phantoms are spheres in a 4D space of 320 × 320 × 15 × 25 (respectively, the x-coordinates, y-coordinates, cardiac phases, and slices). Volume pulsation was added to the phantoms with a linear increase and decrease of the volume with a maximum volume at the eighth cardiac phase. The amount of volume pulsation applied was copied from the actual volume pulsation measured in each of the aneurysms with Analyze. For the aneurysms in Stage II, we used the aneurysm volumes from the primary analysis in Analyze of the improved TFE sequence after contrast enhancement as input for the pulsating phantoms because we assumed that the pulsation quantification on the images after contrast enhancement was the most accurate.

The CNR of each of the aneurysms in our study was determined using the equation included in the Methods section of the article using an ROI in the lumen of the aneurysm and an ROI in the background close to the aneurysm. The SD of the noise was estimated as the SD of the signal of the ROI over the cardiac cycle. This estimation will probably lead to a slightly higher noise level than actually present. Intensity fluctuations in the patient data were estimated at the edge of the aneurysms. First, an ROI (red area in On-line Fig 6) was encoded by eroding all slices in the 3D volume segmentations of the patient data (provided by Analyze) with a flat, disk-shaped structuring element with a radius of 2 voxels, resulting in an eroded ROI. By subtracting the eroded ROI from the segmentation, we determined the edge of the aneurysm (shown in green in On-line Fig 6). The intensity fluctuation (ΔI) was calculated by

$$\Delta I = \frac{[|I(t) - I_\rho|]_o^t max}{I_\mu},$$

where t represents the cardiac phases; $I(t)$, the mean pixel value in the edge of the ROI for phase t; and I_μ, the mean pixel value over all the cardiac phases. The measured intensity fluctuations were applied to the phantoms in a sinusoidal shape, where the measured fluctuation represents the amplitude of that sinus.

The volume pulsation of the pulsating phantom was determined with a signal intensity–based threshold to automatically segment the phantom volume (comparable with the analysis in Analyze but performed in Matlab, as described above). The difference between the volume pulsation input and the volume pulsation output of the phantoms was called the absolute observed artifactual pulsation. The magnitude of the absolute observed artifactual pulsation shows the inaccuracy of the pulsation analysis.

The results of the pulsating phantom analysis of the aneurysms in Stage I of the study show that in all except 2 aneurysms, the imaging analysis overestimated the volume pulsation (On-line Table 2). In Stage II, in all phantoms, the imaging analysis overestimated the volume pulsation (On-line Table 3).

Effect of the Flow Displacement Artifacts on the Accuracy of the Pulsation Analysis

The flow displacement artifacts are another important determinant of the accuracy of the volume pulsation measurement in the patient data. These artifacts are induced by flow in the phase-encoding direction between the time of phase encoding (directly after excitation) and frequency encoding (at t = TE), which causes misregistration. The effect of the flow displacement artifacts on the volume pulsation quantification was estimated from the 3D phase-contrast MR imaging flow velocity data that were available for 6 of the 10 aneurysms included in the current study (Stage I). Briefly, we used the following scan parameters: FOV = 190 × 190 × 20 mm^3 (anterior to posterior × right to left × foot to head), acquired resolution = 0.5 × 0.5 × 0.5 mm^3, TR/TE = 8.5/7.1 ms, flip angle = 20°. A velocity-encoding of 150 cm/s in all directions was used. We obtained 6 cardiac phases, retrospectively gated, using a peripheral pulse unit. The total scan duration was about 13 minutes, depending on the heart rate.

The magnitude of the phase-contrast MR imaging data of a single heart phase was used as a mimic of the aneurysm as seen in the TFE sequence. Subsequently, the following formula was used to calculate the flow displacement artifacts that would be present in the TFE sequence for each voxel of the aneurysm:

$$\Delta y_v = v_y(T_E - t_{pe})$$

where Δy_v represents the artifactual displacement in the phase-encoding direction in a voxel, v_y is the blood velocity in the phase direction, T_E is the echo time (4.4 ms for the TFE sequence), and t_{pe} is the time of phase-encoding (1.6 ms for the TFE sequence, obtained by inspecting the graphical sequence viewer supplied by the MR imaging vendor).

The calculated displacement artifacts were applied to the magnitude of the phase-contrast MR imaging data to simulate the flow-displacement artifacts of the TFE sequence. Because the TFE sequence can be planned in any orientation with respect to the blood flow in the aneurysm, the phase-encoding direction (in which the displacement artifacts occur) was simulated in 3 orthogonal directions, yielding 3 separate estimations of the potential flow-displacement artifacts. Before we applied the displacement to the voxels of the phase-contrast MR imaging magnitude image, this image was interpolated by a factor of 1000 in the simulated phase-encoding direction to allow subvoxel shifts. Minimum aneurysm volume, maximum aneurysm volume, and the pulsation resulting from the flow-displacement artifacts were calculated for all available aneurysms and for the 3 different simulated orientations of the TFE sequence planning.

In 5 of the 6 aneurysms, the pulsation observed because of the flow-displacement artifacts was of the same magnitude or higher compared with the actual pulsation measured in the 6 available patient datasets in at least 1 angulation (On-line Table 5).

REFERENCE

1. Henkelman RM. **Measurement of signal intensities in the presence of noise in MR images.** *Med Phys* 1985;12:232–33 CrossRef Medline

On-line Table 1: Baseline characteristics and pulsation of the 10 unruptured intracranial aneurysms in Stage I

Aneurysm No.	Aneurysm Size, Largest Diameter (Height × Width) (mm)	Age (yr), Sex	Aneurysm Location	Imaging Sequence	Minimum Volume (mm^3)	Moment of Minimum Volume in the Cardiac Cycle (% of Cardiac Cycle)	Maximum Volume (mm^3)	Moment of Maximum Volume in the Cardiac Cycle (% of Cardiac Cycle)	Relative Volume Pulsation (%)	Absolute Volume Pulsation (mm^3)	Absolute Observed Artifactual Pulsation (mm^3)[a]
1	2.8 (1.8 × 1.6)	56, F	Pericallosal	TFE	12	93	15	20	25	3	1.3
2	5.6 (4.5 × 3.9)	60, F[b]	Pericallosal	TFE	70	93	75	53	7	5	1.9
3	6.1 (6.1 × 5.7)	74, F	AcomA	TFE	92	100	98	53	7	6	3.1
4	6.8 (6.0 × 4.7)	60, F[b]	MCA	TFE	56	40	64	13	14	8	0.7
5	8.7 (6.1 × 7.7)	72, F	PICA	TFE	308	7	327	73	6	19	−0.2
6	9.3 (6.6 × 8.2)	56, F	AcomA	TFE	292	100	303	20	4	11	1.1
7	9.6 (6.1 × 9.6)	55, M	MCA	TFE	285	40	298	73	5	13	5.4
8	10.1 (8.8 × 7.7)	64, M	MCA	TFE	276	53	298	13	8	22	−0.4
9	12.9 (12.9 × 6.3)	50, F	MCA	TFE	312	13	324	27	4	12	2.6
10	18.6 (14 × 15.8)	53, F	Basilar	TFE	2078	47	2128	100	2	50	3.5

Note:—AcomA indicates anterior communicating artery.

[a] The absolute observed artifactual pulsation is the difference between the absolute volume pulsation and the volume pulsation of the aneurysm-specific digital phantom and is a measure for the inaccuracy of the volume pulsation analysis (see On-line Appendix for further details).

[b] Two aneurysms in 1 patient.

On-line Table 2: Results of the volume pulsation quantification in pulsating phantoms[a]

	Phantom Input					Phantom Output			
Phantom	CNR	Intensity Fluctuation (%)	Min Volume (mm^3)	Max Volume (mm^3)	Volume Pulsation (mm^3)	Min Volume (mm^3)	Max Volume (mm^3)	Volume Pulsation (mm^3)	Absolute Observed Artifactual Pulsation (mm^3)
1	8	5.7	12	15	3	12.1	16.3	4.3	1.3
2	6	2.4	70	75	5	70.0	76.9	6.9	1.9
3	5	3.2	92	98	6	87.8	96.9	9.1	3.1
4	3	2.9	56	64	8	47.1	55.8	8.7	0.7
5	7	1.8	308	327	19	307.7	326.9	19.2	−0.2
6	6	2.1	292	303	11	292.4	302.3	9.9	1.1
7	3	6.7	285	298	13	276.6	295.0	18.4	5.4
8	1	2.7	276	298	22	276.1	297.7	21.6	−0.4
9	8	2.2	312	324	12	312.8	327.3	14.6	2.6
10	3	2.2	2078	2128	50	1987.8	2034.3	46.5	3.5

Note:—Max indicates maximum; min, minimum.

[a] Phantom numbers correspond with the patients in the Table. The phantom input is the patient data obtained in Stage I of the study. CNR and intensity fluctuations were measured in the patient data and applied to the phantom. The phantom output is the result of the volume analysis of the pulsating phantom (mean of 2 times the analysis in Matlab).

On-line Table 3: Pulsation observed as result of the simulated flow displacement artifacts for 3 different orientations of the acquisition of the TFE sequence (phase-encoding of the TFE sequence parallel to the x, y, or z direction of the phase-contrast MRI dataset, respectively)

Orientation/Pulsation	Aneurysm 1	Aneurysm 2	Aneurysm 3	Aneurysm 4	Aneurysm 5	Aneurysm 6
(1,0,0)						
V_{min} (art in mm^3)	141.4	212.6	174.4	506.0	731.2	596.5
V_{max} (art in mm^3)	148.7	231.8	176.4	509.7	739.1	610.0
$V_{pulsation}$ (art in mm^3)	7.3	19.2	1.9	3.7	7.9	13.5
(0,1,0)						
V_{min} (art in mm^3)	133.9	183.0	179.6	508.6	729.4	591.9
V_{max} (art in mm^3)	139.6	198.8	187.7	511.2	736.1	602.6
$V_{pulsation}$ (art in mm^3)	5.7	15.8	8.1	2.7	6.8	10.7
(0,0,1)						
V_{min} (art in mm^3)	138.1	182.4	179.6	495.1	720.7	588.7
V_{max} (art in mm^3)	142.6	188.8	185.2	506.8	732.5	600.0
$V_{pulsation}$ (art in mm^3)	4.5	6.4	5.6	11.7	11.7	11.2
Actual pulsation, aneurysm size[a]						
Aneurysm size (mm)	5.6	6.1	6.8	9.6	10.1	12.9
V_{min} (mm^3)	136.9	193.8	182.1	506.5	733.5	599.6
$V_{pulsation}$ (mm^3)	5	6	8	13	22	12

Note:—art indicates artifacts; V_{max}, maximum aneurysm volume; V_{min}, minimum aneurysm volume; $V_{pulsation}$, pulsation volume.

[a] The actual pulsation as measured in the patient data (Stage I) and the aneurysm size.

On-line Table 4: Baseline characteristics and pulsation of the 9 unruptured intracranial aneurysms in Stage II

Aneurysm No.	Aneurysm Size, Largest Diameter (Height × Width) (mm)	Age (yr), Sex	Aneurysm Location	Imaging Sequence	Minimum Volume (mm^3)	Moment of Minimum Volume in the Cardiac Cycle (% of Cardiac Cycle)	Maximum Volume (mm^3)	Moment of Maximum Volume in the Cardiac Cycle (% of Cardiac Cycle)	Relative Volume Pulsation (%)	Absolute Volume Pulsation (mm^3)	Absolute Observed Artifactual Pulsation (mm^3)[a]
11	2 (2 × 1.6)	53, F	MCA	TFEi	3	22	4	6	73%	2	–
				CE TFEi	2	22	3	94	36%	1	2
12	6.2 (5.1 × 3.3)	58, F	MCA	TFEi	68	28	90	6	31%	21	–
				CE TFEi	96	33	104	6	8%	8	1
13	5.4 (4.8 × 4.4)	70, M	AcomA	TFEi	44	78	75	100	70%	31	–
				CE TFEi	78	78	96	100	23%	18	13
14	5.7 (5.7 × 3.1)	47, F	MCA	TFEi	62	28	79	94	28%	17	–
				CE TFEi	70	22	78	89	11%	8	9
15	8.7 (8.1 × 6)	39, M	MCA	TFEi	134	83	153	17	14%	19	–
				CE TFEi	NA	NA	NA	NA	NA	NA	NA
16	8.7 (7.9 × 5.4)	70, M	AcomA	TFEi	91	72	149	94	64%	58	–
				CE TFEi	114	72	138	100	22%	25	27
17	9.4 (8.7 × 6.7)	53, M	AcomA	TFEi	188	89	215	11	14%	27	–
				CE TFEi	256	83	265	100	4%	9	10
18	12.3 (8.1 × 8)	70, M	AcomA	TFEi	206	78	289	94	41%	84	–
				CE TFEi	166	78	191	94	15%	25	24
19	13.7 (10.9 × 8.7)	51, M	AcomA	TFEi	419	22	507	89	21%	88	–
				CE TFEi	581	22	603	94	4%	22	25

Note:—NA indicates not applicable; TFEi, the improved version of the turbo field echo sequence to image pulsation used in Stage II; AcomA, anterior communicating artery; CE, contrast-enhanced.

[a] The absolute observed artifactual pulsation is the difference between the absolute volume pulsation and the volume pulsation of the aneurysm-specific digital phantom and is a measure for the inaccuracy of the volume pulsation analysis (see On-line Appendix for further details). Only the contrast-enhanced TFE data were used as input for the phantom experiment because we expected the contrast-enhanced TFE sequence to perform better than the improved TFE alone.

On-line Table 5: The results of the volume pulsation quantification in pulsating phantoms of Stage II[a]

	Phantom Input					Phantom Output			
Phantom	CNR	Intensity Fluctuation (%)	Min Volume (mm^3)	Max Volume (mm^3)	Volume Pulsation (mm^3)	Min Volume (mm^3)	Max Volume (mm^3)	Volume Pulsation (mm^3)	Absolute Observed Artifactual Pulsation (mm^3)
11	19	24	2	3	1	2	4	2	1
11[b]	44	22	2	3	1	1	4	3	2
12	29	20	96	104	8	93	102	9	1
12[b]	34	12	96	104	8	96	105	9	1
13	25	38	78	96	18	77	108	32	14
13[b]	19	24	78	96	18	73	104	31	13
14	18	22	70	78	8	68	84	16	9
14[b]	29	13	70	78	8	68	85	17	9
15	–	–	–	–	–	–	–	–	–
15[b]	–	–	–	–	–	–	–	–	–
16	39	30	114	138	25	113	164	50	26
16[b]	24	21	114	138	25	113	164	51	27
17	22	16	256	265	9	263	283	21	12
17[b]	23	10	256	265	9	263	282	19	10
18	19	18	166	191	25	156	203	47	22
18[b]	19	7.5	166	191	25	155	204	49	24
19	14	15	581	603	22	593	637	44	22
19[b]	28	8	581	603	22	553	600	47	25

Note:—Max indicates maximum; min, minimum.

[a] Phantom numbers correspond with the patients in On-line Table 1. The phantom input is the patient data obtained in Stage II of the study. The aneurysm volumes from the primary analysis in Analyze of the improved TFE sequence after contrast enhancement were used as input for the pulsating phantoms because we assumed that the pulsation quantification on the images after contrast-enhancement was the most accurate. CNR and intensity fluctuations were measured in the patient data and applied to the phantom. The phantom output is the result of the volume analysis of the pulsating phantom (mean of 2 times the analysis in Matlab).

[b] The phantom with the improved TFE sequence after contrast enhancement. In aneurysm 5, the image acquisition of the contrast-enhanced improved TFE failed; therefore, we were not able to perform a phantom analysis.

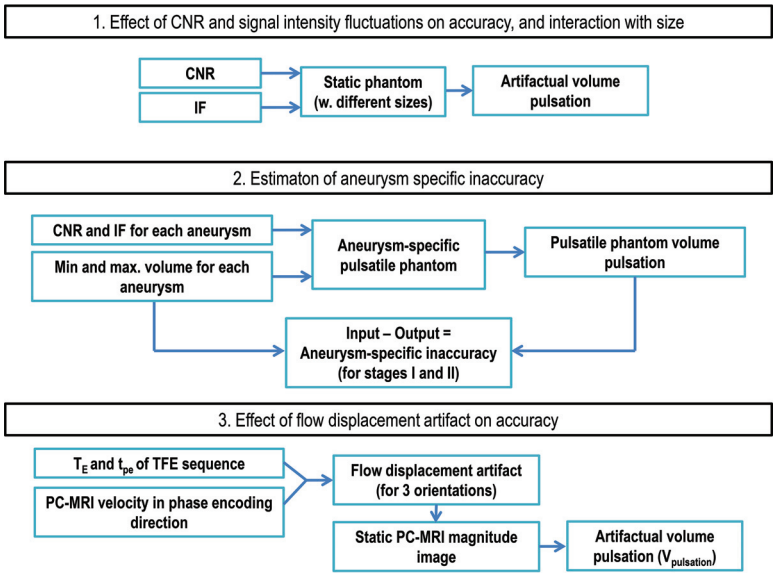

ON-LINE FIG 1. Schematic overview of the accuracy analysis of the volume pulsation quantification. IF indicates intensity fluctuation; min, minimum; max, maximum; PC-MRI, phase-contrast MR imaging; T_E, echo time; T_{pe}, time of phase-encoding; $V_{pulsation}$, pulsation volume.

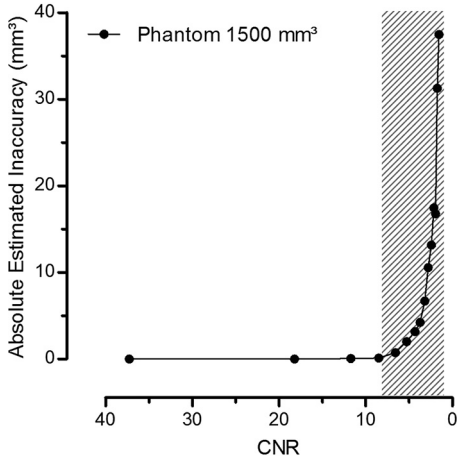

ON-LINE FIG 2. Estimated inaccuracy of the volume pulsation analysis as a function of the contrast-to-noise ratio. Measurement points indicate the decreasing CNR values as applied to the static phantom. The *shaded area* indicates the range of temporal CNRs measured in the patient scans of Stage I, indicate the range of CNR values that is relevant for interpreting the results of the patient study.

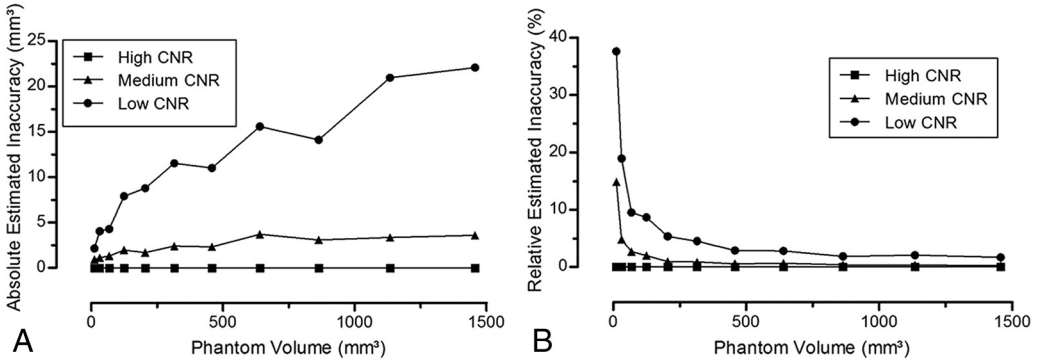

ON-LINE FIG 3. The interaction of the size of the phantom with the CNR on the estimated inaccuracy of the volume pulsation measurement. The estimated inaccuracy is plotted against phantom volume in the static phantoms for 3 discrete CNRs, namely high CNR (CNR≈12), medium CNR (CN≈4), and low CNR (CNR≈2). *A*, The influence of volume on the absolute estimated inaccuracy (cubic millimeters). *B*, Influence of volume on the relative estimated inaccuracy (percentage).

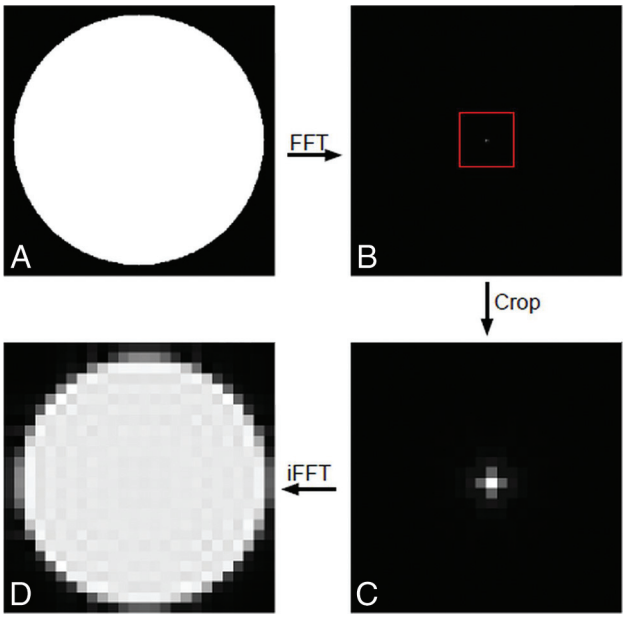

ON-LINE FIG 4. Simulation of the partial volume effect in the phantom. *A*, High-resolution phantom. *B*, Magnitude image of the frequency domain after applying the fast Fourier transform. The *red square* indicates the cropping area containing the low spatial frequencies. *C*, Magnitude image of the frequency domain cropped back to the correct resolution. *D*, Normal-resolution phantom shows a clear partial volume effect, after applying the inverse fast Fourier transform. FFT indicates fast Fourier transform; iFFT, inverse fast Fourier transform.

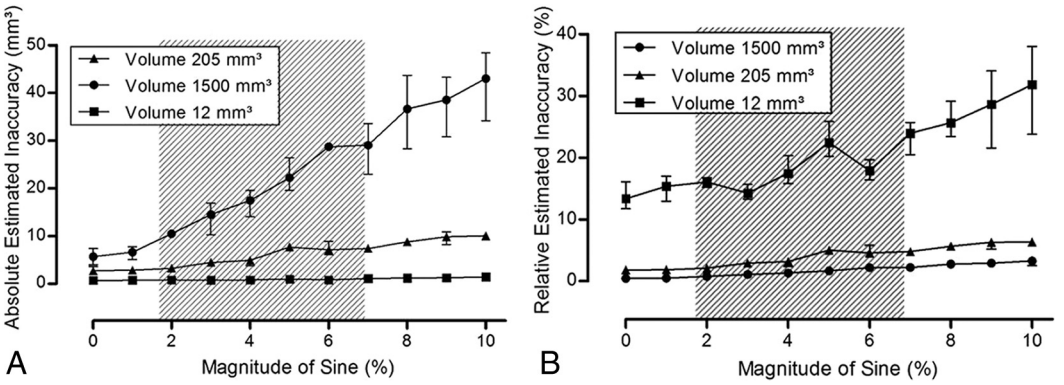

ON-LINE FIG 5. Estimated inaccuracy of the volume pulsation analysis as a function of the signal intensity fluctuations. The estimated inaccuracy of the analysis method was defined as the amount of observed pulsation in a static digital phantom: absolute estimated inaccuracy versus the magnitude of sinusoidal brightness fluctuation in percentages of the mean signal (*A*) and relative estimated inaccuracy (relative is obtained by normalizing to mean volume) versus the sinusoidal brightness fluctuation in a simulated high-quality scan (CNR≈12) for 3 different phantom sizes (*B*). *Shaded area* indicates the range of brightness fluctuations measured in the patient scans in Stage I of the patient study, to indicate the range of signal intensity fluctuation values that is relevant for interpreting the results of the patient study.

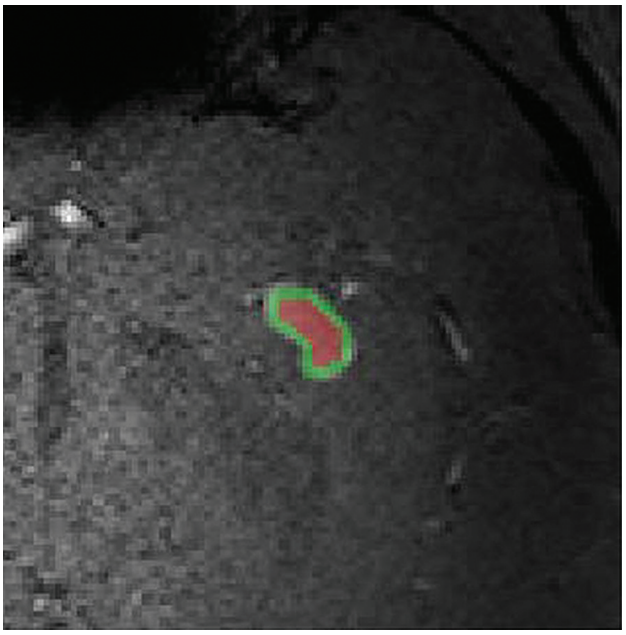

ON-LINE FIG 6. Intensity fluctuation measurement. A slice through a middle cerebral artery aneurysm with the eroded ROI in red and the residual edge of the aneurysm in green.